

**NATuRal instability of semiConductors thIn SOLid films for sensing and photonic applications** *Horizon 2020*

Project title: **NATuRal instability of semiConductors thIn SOLid films for sensing and photonic applications (NARCISO)**

Grant Agreement: 828890

Call identifier: H2020-FETOPEN-2018-2020/H2020-FETOPEN-2018-2019-2020-01

Start Date of Project: 01/03/2019

Duration: 36 months

Deliverable D.1.3 – V1.0**Title: Report on characterizations of the assisted dewetting materials**

Leader partner	CNR
Author(s)	Monica Bollani
Estimated delivery	31/7/2021
Actual delivery	
Revised version	
Work Package	WP1
Tasks	1.3
Dissemination level	Public
Version	1.0

Disclaimer

The content of this deliverable does not reflect the official opinion of the European Union. Responsibility for the information and views expressed herein lies entirely with the author(s).



Contents

Contents	2
1. Introduction	3
2. Assisted dewetting instability on SOI or GOI samples	3
2.1 Templated dewetting of single-crystal nanowires	3
2.2 Effect of annealing temperature and patch size on assisted Si based dewetting:	6
2.3 Sharp Si-based dielectric resonators.....	7
3 Conclusions	12



1. Introduction

This document is a deliverable of the NARCISO project which is funded by the European Union's H2020 Programme under Grant Agreement (GA) No. 828890.

This deliverable is focus on description of the results achieved on characterizations of the assisted dewetting materials using pure Si, pure Ge or SiGe alloys as original films. We show that the underlying instability of the patterned thin semiconductor film under annealing can be perfectly controlled to form monocrystalline, complex nanoarchitectures extending over several microns. These complex patterns are obtained guiding the dewetting fronts by etching ad-hoc patches prior to annealing. They can be reproduced over hundreds of repetitions extending over hundreds of microns.

2. Assisted dewetting instability on SOI or GOI samples

During dewetting, under the action of surface diffusion, mass is accumulated in a thick, receding rim at the film edges (where the curvature of the film is large), which eventually becomes unstable and evolves in elongated structures (fingers). When other instabilities, such as corner instability, bulging, rim pinch-off and faceting, take place the film breaks in isolated, monocrystalline, faceted islands. The intricacies of these instabilities are further modified by the presence of preferential directions for mass transport, which must be considered to explain this complex dewetting scenario. For example, it is well known that for a (001) oriented UT-SOI (ultra-thin silicon on insulator) the dewetting speed along the [100] in-plane direction is much larger than that in the [110] direction. These dewetting fronts are thus respectively called "unstable" and "stable". A viable method for enhancing the level of ordering of the dewetted Si and SiGe structures relies on pre-patterning the thin film prior to annealing. Our approaches are based on e-beam lithography (EBL), photolithography and laser writing processes for creating small patches in the ultra-thin SOI or SGOI.

2.1 Templated dewetting of single-crystal nanowires

We fabricate arrays of in-plane, ultra-long nano-wires (up to 0.75 mm) and complex inter-connected circuits of monocrystalline silicon using a catalyst- and epitaxy-free, hybrid top-down/bottom-up approach based on the natural morphological evolution of thin solid films. Here, we tested the stability against annealing of a 12 nm thick UT-SOI (at temperature between 720 and 775 °C, for periods ranging from 15 min to 2 h) patterned by EBL and reactive ion etching (RIE) in long trenches with variable pitch ($d_{LL} = 0.5$ up to 4 μm) defining patches featuring a width w ranging from ~ 400 nm up to ~ 3.8 μm . The final structures have a lateral size up to five times smaller than the etched patch width, are obtained with size- and position-control and are electrically-isolated from the substrate. [For the sample preparation method see M. Bollani et al, *Nature Communications* (2019) 10:5632].

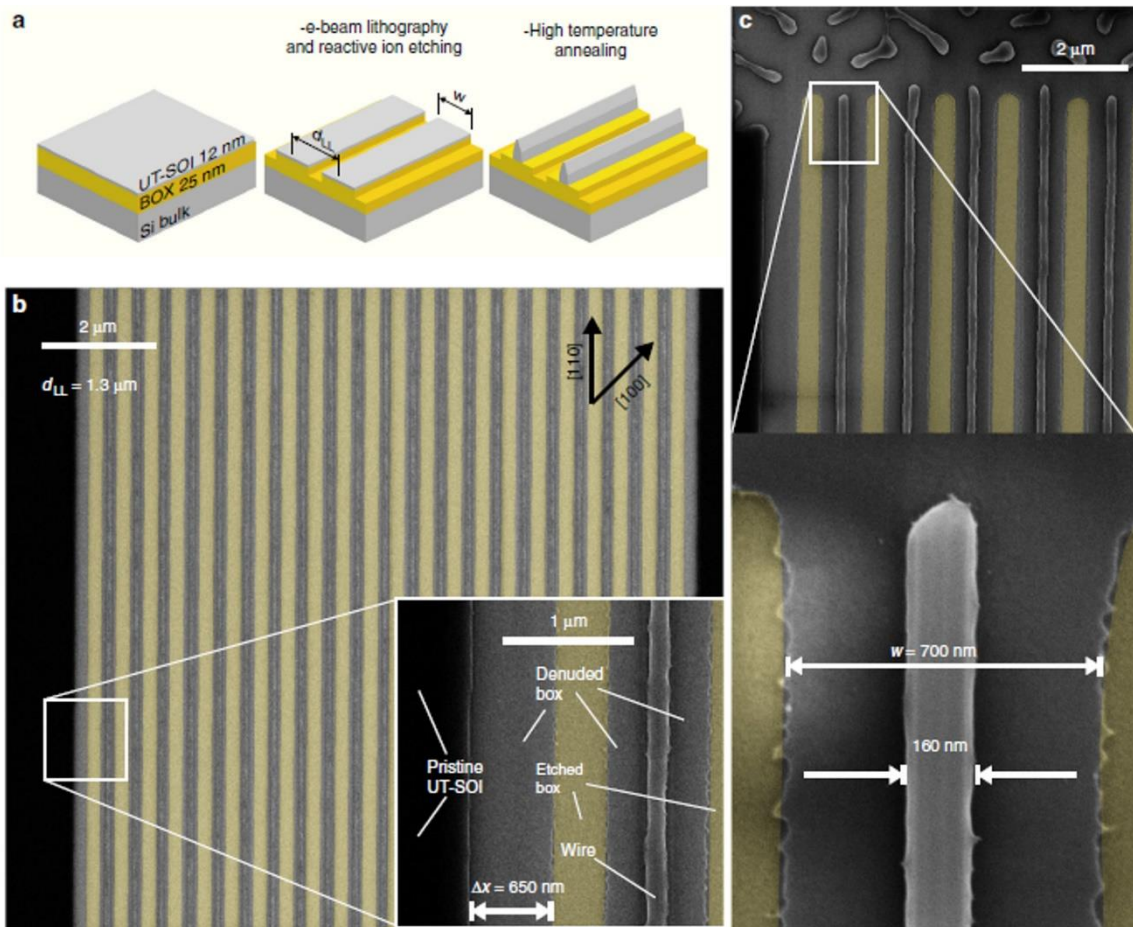
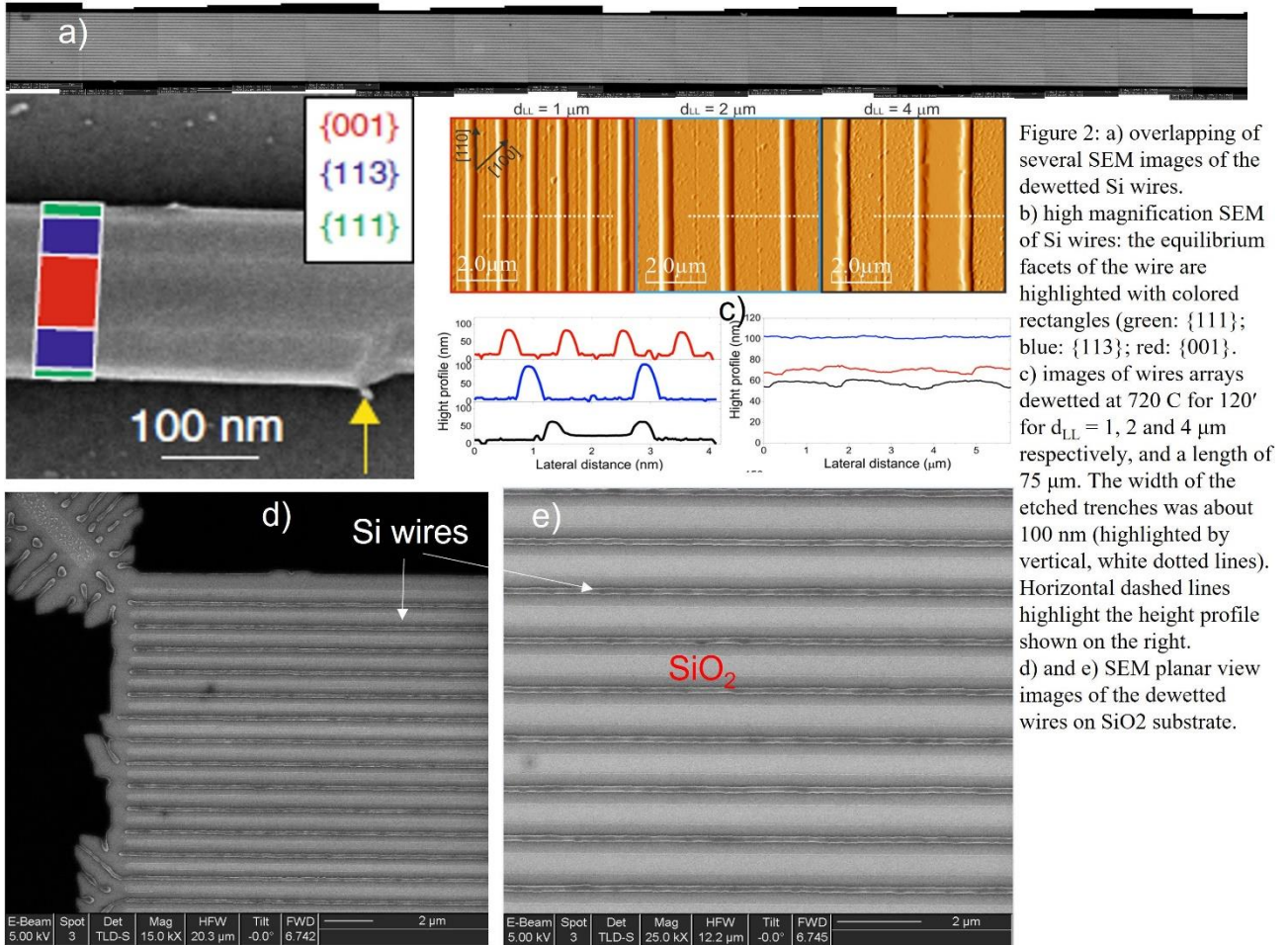


Fig. 1 a) Scheme of the sample fabrication: long patches are created in a 12 nm thick ultra-thin silicon on insulator (UTSOI) on buried oxide with a pitch of d_{LL} and width w . b) SEM image of 21 parallel nano-wires of length 0.75 mm, $d_{LL}=1.3 \mu\text{m}$, and $w=700 \text{ nm}$. The yellow areas highlight the etched trenches. Bottom right inset blow up of a free-propagating edge and a dewetted wire. c) Top panel: detail of the extremity of the wires. Bottom-right panel: blow-up of a wire extremity.

In optimized conditions (annealing temperature and time, and patterns width) we observe the formation of extremely long wires, with a length limited only by the patch design (up to 0.75 mm, Figure 1). Wires with no breaks and perfectly homogeneous height and width over their full length can be formed with a 100% success rate. All the UT-SOI available in the patch ($w = 700 \text{ nm}$) collapsed in individual wires featuring a base of about 160 nm (~ 4 times smaller than w) and a height of 50 nm. In these conditions of annealing temperature and time, a simple stable dewetting front freely receding (semi-infinite UT-SOI) covers a distance of about $\Delta x = 650 \text{ nm}$, a length comparable to the overall patch width w . Several scanning electron microscopy characterizations have been carried out, showing the morphological evolution of the wires and the presence of atomically flat facets (Figure 2 a-e). In order to rule out the presence of crystalline defects in the dewetted structures we performed atomic-resolution scanning transmission electron microscopy (STEM) imaging on a wire (Figure 2 f-g). In line with previous evidences in Si- and SiGe-based islands TEM analyses, we observe

for the wires structures the typical crystalline structure of bulk Si and the absence of extended dislocations. A slight crystalline disorder can be observed in some part of the wire body, at the interface with the original UT-SOI substrate (at about 12 nm from the BOX, figure 5 f-g). We ascribe this feature to residual defectivity on the UT-SOI substrate, possibly due to a non ideal cleaning of the surface.



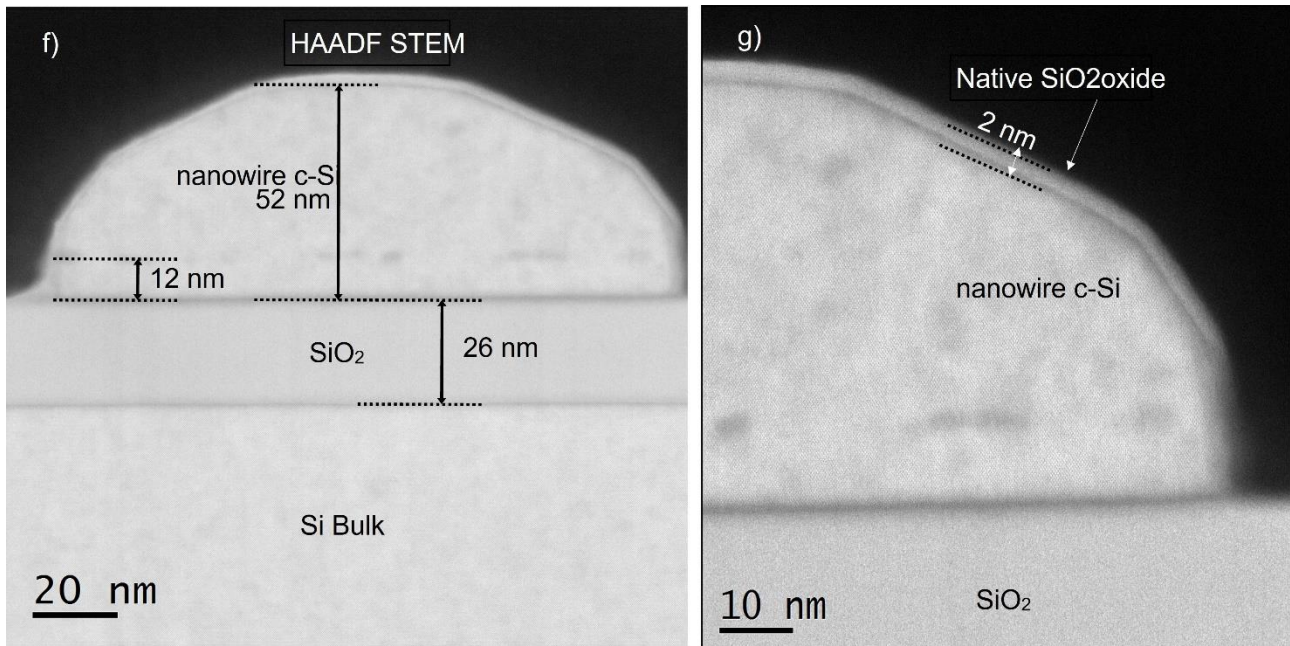


Figure 2 f-g: scanning transmission electron micrograph (STEM) of the section of a dewetted wire.

2.2 Effect of annealing temperature and patch size on assisted Si based dewetting:

For other studies, the etched patch shapes are simple squares (with side ranging from 500 nm up to 5 μm) and large square patches (5 μm) with additional features etched within them (e.g. holes, dashes, crosses, etc.) by means of EBL and RIE. We first address the effect of the annealing temperature on the final outcome of large and complex, squared patches. A precise and reproducible ordering of the dewetted structures is only possible using annealing temperature below $\sim 750^\circ\text{C}$. To highlight this point, we analyze dark-field images of some samples (annealed at 720°C for 3 h) and other samples (annealed for 800°C for 1 h). The bright scattering spots observed in dark field images correspond to individual islands (Figure 3). More precisely, we provide that these objects are resonant antennas and different colours are attributed to resonant electromagnetic modes confined in each island. These spectral resonances reflect their specific size, shape and composition and thus constitute a precise probe of the islands' homogeneity.

For low-temperature annealing, we assist to the formation of a few large islands, eventually exhibiting multi-modal size distributions, with a rather good reproducibility of the complex arrangement over several repetitions. Differently from the low temperature case (Figure 3a), at high temperature the dewetting cannot be controlled and a random organization of many small islands is observed (Figure 3 b). This feature reminds the typical results obtained via spontaneous dewetting of the same UT-SOI in non-patterned areas. In these experimental conditions (device thickness 12 nm and low annealing temperature, $\sim 720^\circ\text{C}$) the typical length of the underlying dewetting

instability leads to isolated islands which are ~ 800 nm distant one from the other. [M. Abbarchi et al. *Microelectronic Engineering* 190 (2018) 1–6].

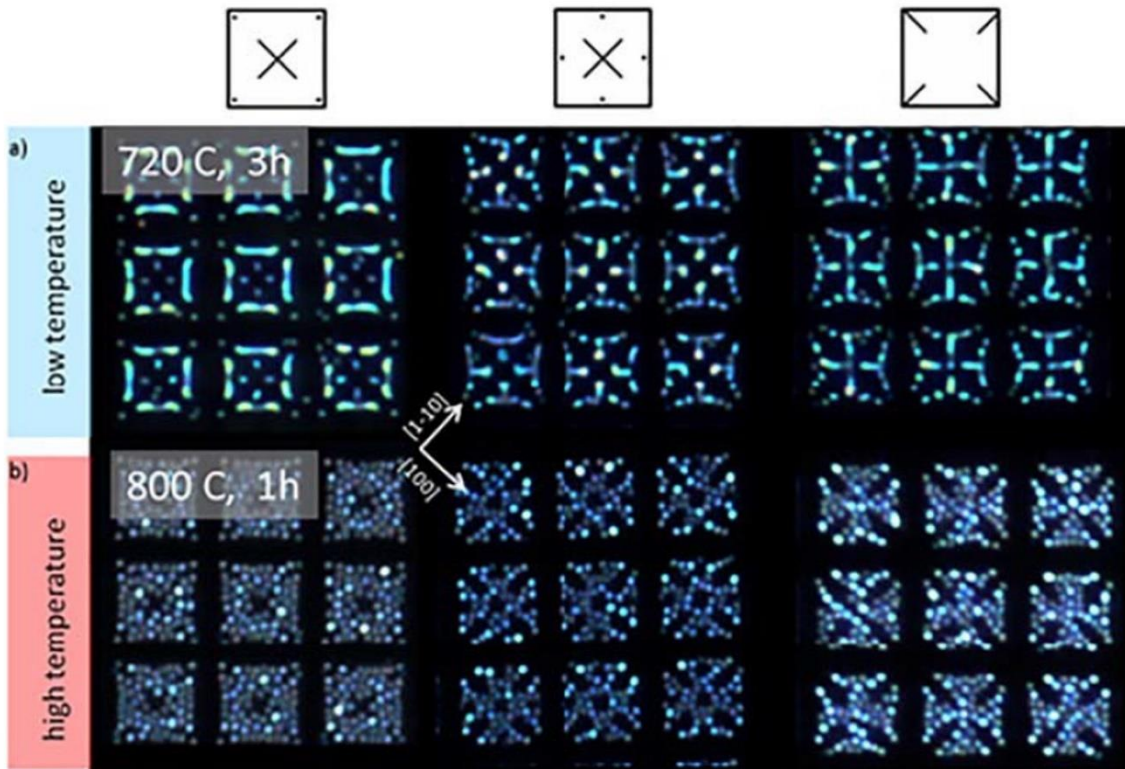


Figure 3. Role of temperature. a) Optical microscope dark field images of 3×3 repetitions of dewetted complex patterns for low temperature annealing (720 °C for 3 h). The full pattern includes 12×12 identical repetition of the same patch shape. b) Same as a) for high temperature annealing (800 °C for 1 h). The top insets display the initial patch shape etched via EBL & RIE before annealing.

2.3 Sharp Si-based dielectric resonators

The main goal of these experiments has been to obtain well-defined nanostructures by using the solid state dewetting and test their optical response. Mie resonators are all-dielectric antennas with reduced absorption losses and high permittivity which make them an ideal candidate for light-matter interaction and light manipulation, potentially enriching the current performances of photonic devices.

Here we report the results achieved to tune a defined structural color exploiting the resonances of Mie resonators sitting atop a thick SiO_2 , responsible of a sharp photonic modulation. For these templates, the optical lithography and reactive ion etching have been used. Once the pattern is completed, the samples have been inserted in the ultra-high vacuum of the MBE chamber to perform the annealing. The silicon nano-islands' far-field scattering intensity is coupled with the etalon effect. The efficiency of the Mie scattering out-couples the light interfering with the etalon depending on the nano-islands' size and drives the light at smaller angles compared to the one from

the incident beam. Finally, we got colors that cover the visible spectrum along with resonances with the contrast between min and max of the intensity. Specifically, the mono-crystalline, silicon on insulator (SOI) is a single-crystal (001) film, 125 nm thick atop 2 μm thick SiO₂ layer (buried oxide, BOX) on a bulk Si (001) wafer (Figure 4a).

It is thinned to 20 nm SOI by rapid thermal oxidation (RTO) at 950 °C in O₂ atmosphere for 3 hours in order to transform the top part of the SOI in SiO₂. By dipping the oxidized samples in a HF-solution at 5% in de-ionized water (95%) the top SiO₂ layer is removed thus exposing the remaining bottom SOI. Island fabrication is performed in two steps: 1) patterning by photolithography and 2) solid state dewetting via high temperature annealing. At the end of the dewetting process we obtain monocrystalline and atomically smooth islands featuring the typical facets of the equilibrium shape of silicon (Figure 4 b). Large islands arrays (Figure 4c) can be fabricated with controlled size (base diameter from about 280 to 780 nm) and regular organization (Figure 4 d). The similar scattering color accounts for a good homogeneity, as also confirmed by the small fluctuation obtained by measuring the base size of several islands for each pitch. Island's height is in the 90 to 150 nm range, depending on the initial pitch size. Smaller island size (e.g. featuring bright scattering at visible frequency) can be obtained by reducing the pitch of the lithographic step.

For optical spectroscopy at visible frequency (owing to the limits of our silicon-based detector) we chose a set of dewetted islands with increasing base diameter, from about 100 to 200 nm (Fig. 5 a, left column). Slight shape asymmetries observed in some islands are ascribed to a non-complete dewetting that did not lead to the final equilibrium shape of silicon crystals. In principle, these defects could be improved with a longer annealing time or a higher temperature. Dark field images reveal a net colorization from blue to red, when increasing particle size (Figure 5 a, right column). The corresponding scattering spectra (normalised by the white lamp used for illumination) confirm this tendency, showing several sharp bands that increase in number at long wavelength for larger islands (Figure 5 b). These resonances share a similar spectral position and spacing between them, although some differences (up to 25-30 nm) are observed. These differences can be accounted for by imperfections in the etching (locally thicker or thinner BOX), incomplete dewetting leaving some pristine c-UT-SOI nearby the islands, residual Si particles on the BOX nearby the islands, intermixing of Si and SiO₂, and asymmetries in the dewetted islands. By these studies, we confirm that a low resolution etching method joined with solid-state dewetting can provide ordered arrays of monocrystalline Si-based islands with size control and featuring a bright Mie scattering in the visible

spectral

range.

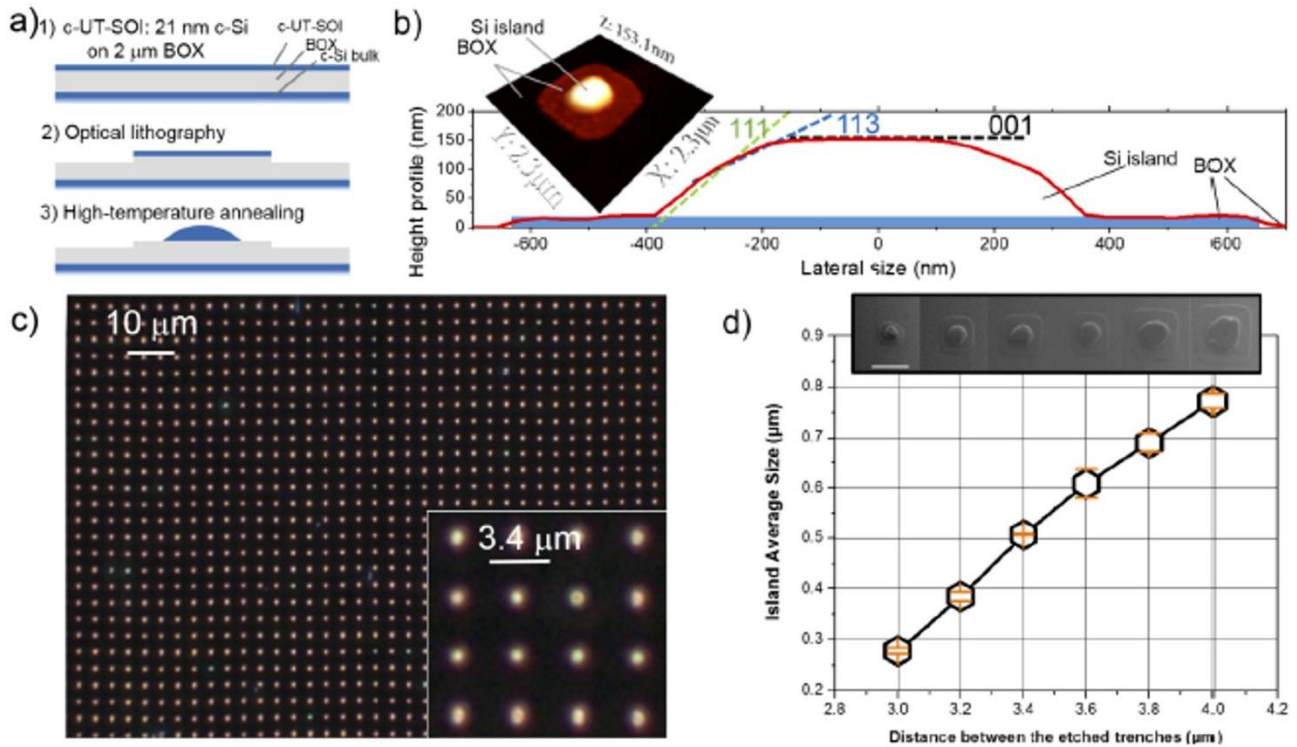


Figure 4) Scheme of the main fabrication steps. 1) SOI with 21 nm of monocrystalline Si (c-Si) ad device on 2 μm of silicon oxide (buried oxide, BOX). 2) Optical lithography and plasma etching. 3) High temperature annealing in ultra-high vacuum. b) AFM profile of an individual island. The main crystal facets are highlighted. The inset shows a 3D representation of the island. c) Optical dark-field image of a typical array of organized dewetted Si islands. The inset shows the homogeneity of the islands obtained with a periodicity of 3.4 μm. d) Average island size as a function between the etching pitch as obtained by scanning electron micrographs (SEM). The error bar represents the standard deviation. The line is a guide for the eyes. The top inset show a typical SEM for each etched pitch.

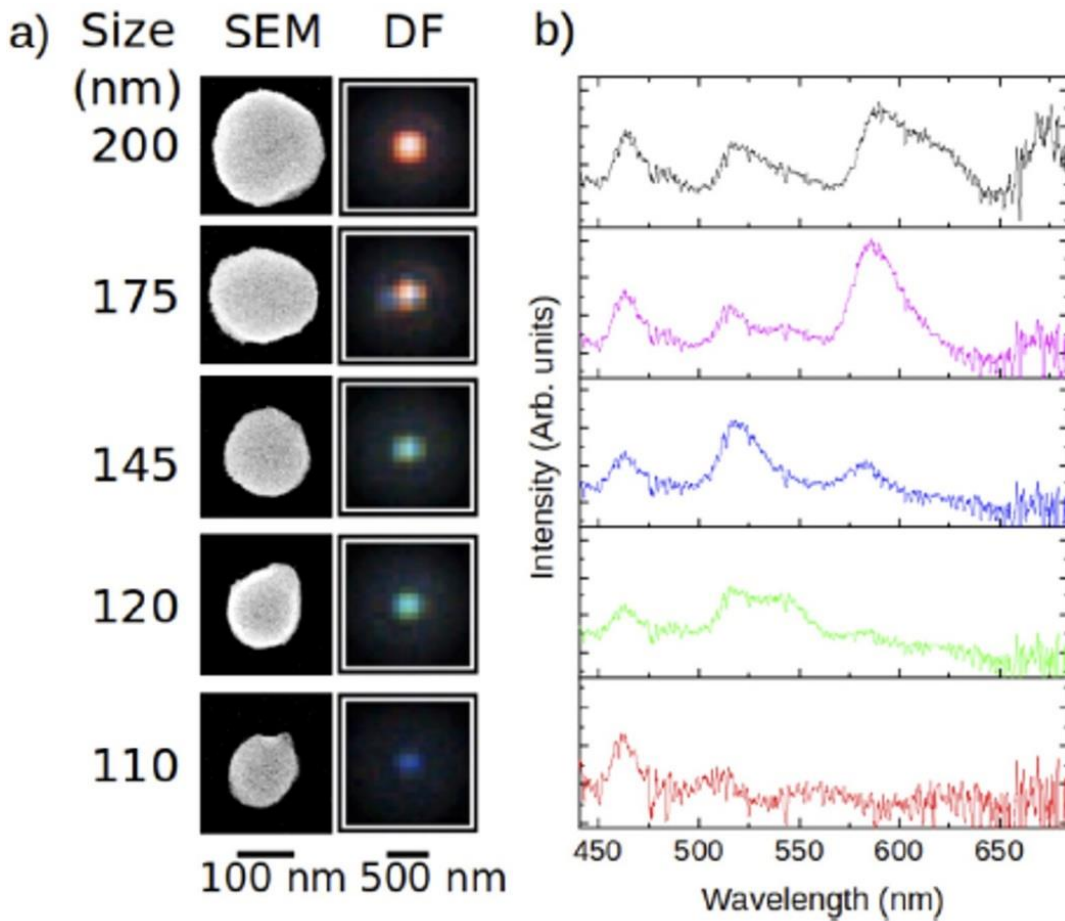


Figure 5 a) Left column: SEM images of crystalline Si dewetted islands. Their corresponding size is highlighted at their left. Right panel: dark-field optical microscope images of the islands shown in the left column. b) Dark-field scattering spectrum corresponding to the islands shown in a).

Similar templates are realized also by e-beam lithography and reactive ion etching, and then characterized by SEM and scanning near-field optical spectroscopy. The investigated samples consist in monocrystalline Si-based islands and Si_{70%}Ge_{30%} followed by solid state dewetting. A 2 μm thick layer of SiO₂ separates the islands from an underlying bulk Si substrate. In Figure 6 we report a top view SEM image of the sample showing several islands; the details of a single island with a diameter of the order of 300nm can be observed in the SEM image of the inset of figure 6 a. A commercial scanning near-field optical microscope (SNOM) in collection geometry is used in order to detect the near-field scattered emission of a single island under a tilted illumination configuration (as shown in the sketch of figure 6 b). The spatially resolved optical maps are recorded by scanning the probe dielectric tip over the sample at a fixed distance (few tens of nm). The employed illumination source, tilted of an angle $\theta=30^\circ$ with respect to the perpendicular axis of the scatterer, is a Supercontinuum laser whose emission spectrum is reported in figure 6 c, ranging mainly in the

wavelength interval (500-800) nm. Then the collected signal is dispersed by a spectrometer and collected by a cooled Si-based CCD camera. At every tip position, the entire spectrum of the sample is collected with a spectral resolution of 0.1 nm. The whole technique therefore allows to perform hyper spectral imaging, that is we collect a full near-field spectrum of a system for any spatial pixel of the near-field map.

A systematic near-field study is in progress showing how the modes arising from the combination of the Mie resonances of an all-dielectric dewetted island with the etalon effect. By means of Finite Difference Time Domain (FDTD) simulations we are achieving a full comprehension of the sensitivity of magnetic light with respect to the thickness of the substrate and the angle of illumination (*a dedicated paper is progress*). Theoretical and experimental results are crossed in order to obtain a

detailed analysis of how such sensitivity affect the near-field emission pattern and beam steering properties of the assisted dewetted Si-based antenna, providing relevant features for future optoelectronic and quantum applications.

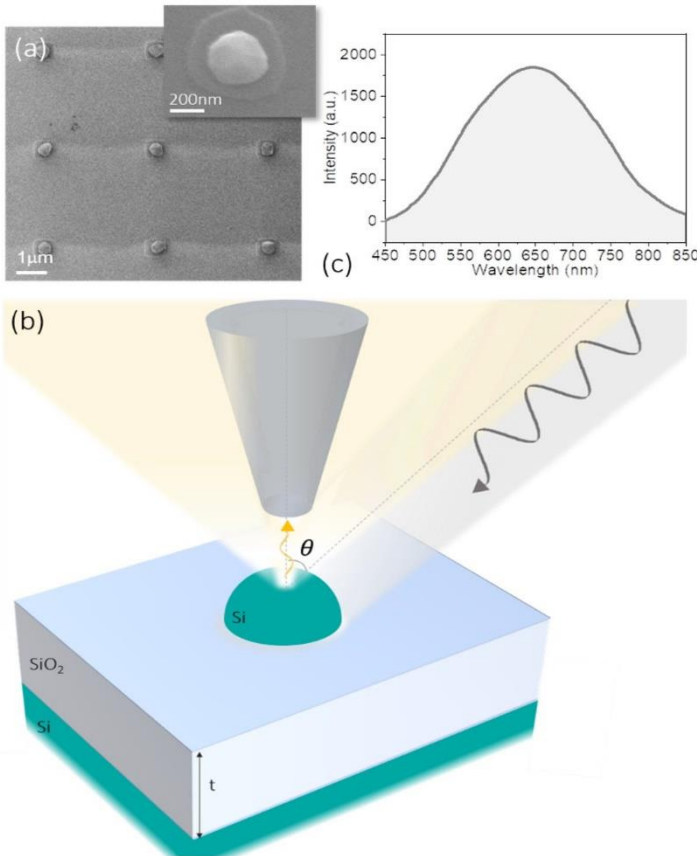


Figure 6: (a) Top view SEM image of the sample, in which several dewetted islands are shown. The inset displays the magnified SEM image of a single island. (b) Sketch of the experimental set up: the tilted illumination (of an angle θ with respect to the axis perpendicular to the sample) from the Supercontinuum is scattered by the island. The yellow cone is a representation of the angular pattern of scattering. The scattered light is collected by the near-field tip at a distance of ≈ 10 nm. (c) Emission spectrum of the Supercontinuum source detected by a Si-based CCD camera.



3 Conclusions

In this deliverable we report the optimization and validation of the dewetting processes on template substrates. By e-beam lithography the maximum writing field is $1 \times 1 \text{ cm}^2$, whereas by optical lithography it is possible in principle to create larger patterns (with areas up to 4 inches with the mask aligners present in the network). Thus, we demonstrated that optical lithography is a perfectly adapted tool to form monocrystalline Si (D. Toliopoulos, Vol. 28, No. 25 / 7 December 2020) and Ge islands (to be published). In addition to this, we were able to avoid the use of ultra-high vacuum (in a molecular beam reactor) showing well-ordered dewetted islands using secondary vacuum ($\sim 10^{-6}$ torr) in a conventional rapid thermal processor (to be published). Also in these cases, NARCISO network has demonstrated and validated the control of the dewetting instability on template substrates by a combination of optical (light reflection, transmission, scattering, near and far field) and microscopic (AMF, TEM, SEM) characterizations.